NASA TM-80105

NASA Technical Memorandum 80105

AN EXPLORATORY STUDY OF A FINITE DIFFERENCE METHOD FOR CALCULATING UNSTEADY TRANSONIC POTENTIAL FLOW

Robert M. Bennett and Samuel R. Bland

June 1979

NASA

National Aeronautics and
Space Administration

Langley Research Center
Hampton, Virginia 23665

1 Report No NASA TM 80105	2 Government Accession No	3 Recipient's Catalog No
4 Title and Subtitle AN EXPLORATORY STUDY OF A FINITE DIFFERENCE METHOD FOR CALCULATING UNSTEADY TRANSONIC POTENTIAL FLOW		5 Report Date June 1979
		6 Performing Organization Code
7 Author(s) Robert M. Bennett and Samuel R. Bland		8 Performing Organization Report No
9 Performing Organization Name and Address NASA Langley Research Center Hampton, VA 23665		10 Work Unit No 505-02-23-01
		11 Contract or Grant No
12 Sponsoring Agency Name and Address National Aeronautics and Space Administration Washington, DC 20546		13 Type of Report and Period Covered Technical Memorandum
		14 Sponsoring Agency Code

15 Supplementary Notes

16 Abstract

A method for calculating transonic flow over steady and oscillating airfoils has been developed by Isogai. It solves the full potential equation with a semi-implicit, time-marching, finite difference technique. Steady flow solutions are obtained from time asymptotic solutions for a steady airfoil. Corresponding oscillatory solutions are obtained by initiating an oscillation and marching in time for several cycles until a converged periodic solution is achieved. In this paper the method is described in general terms and results for the case of an airfoil with an oscillating flap are presented for Mach numbers 0.500 and 0.875. Although satisfactory results are obtained for some reduced frequencies, it is found that the numerical technique generates spurious oscillations in the indicial response functions and in the variation of the aerodynamic coefficients with reduced frequency. These oscillations are examined with a dynamic data reduction method to evaluate their effects and trends with reduced frequency and Mach number. Further development of the numerical method is needed to eliminate these oscillations.

17 Key Words (Suggested by Author(s)) Unsteady flow Transonic flow Finite difference methods	18 Distribution Statement Unclassified – Unlimited Subject Category 02	
19 Security Classif (of this report) Unclassified	20 Security Classif (of this page) Unclassified	21 No of Pages 20	22 Price* $4.00

INTRODUCTION

The flutter critical portion of the aircraft flight envelope generally occurs at transonic speeds. This critical condition results from both the high dynamic pressures of operation and the dip in flutter speed or "bucket" that occurs at transonic Mach numbers. The dip in flutter speed is influenced by airfoil thickness and shape and cannot be satisfactorily treated by state-of-the-art aerodynamic analyses. Thus an important current topic in aerodynamic research is the development of methods for the calculation of unsteady aerodynamics for use in transonic flutter analysis. Many of the current efforts have built on the recent success of steady flow numerical finite difference solution procedures and, to date, have primarily been applied to two-dimensional airfoils as a means of evaluating and refining the analyses and algorithms involved. One such method of solving the full potential equation was presented in reference 1. It has been extended by Isogai (unpublished) and has been applied to calculate several examples of unsteady transonic flow (references 2-3). In general, comparisons with other methods were favorable (references 1-2). One exception was that strong shocks were located further aft on the airfoil than corresponding Euler equation solutions (ref. 1). This trend might be anticipated since the full potential equation overpredicts the strength of shock waves (ref. 4). Similar comparisons with experimental data of references 5 and 6 for the NACA 64A006 airfoil with an oscillating flap were also in reasonable agreement (references 2-3) considering the fact that the theory did not allow for viscous or wind tunnel effects.

To define the variation of aerodynamic forces with reduced frequency for a transonic flow, the forces were calculated using Isogai's method for a moderate set of k-values and for a Mach number of 0.875 (ref. 3). Results of these calculations showed oscillations in the variation of the forces with k which were particularly pronounced for reduced frequencies less than 0.10. In this paper a more extensive set of calculations are presented for a Mach number of 0.500 along with the previous results for a Mach number of 0.875. The oscillatory behavior of the coefficients with k is shown to exist also at the lower Mach number. The oscillations are believed to be spurious and generated by the numerical method. Corresponding indicial response functions for flap displacement are also presented. They are analyzed by the dynamic data reduction method of reference 7 in an effort to define further and to evaluate the effects of the oscillations and their trends with Mach number. Other calculations are also discussed in which the finite difference grid and the time step were varied in order to define more precisely the source of the oscillations.

NOMENCLATURE

a   (speed of sound)/V_∞

a_∞ (freestream speed of sound)/V_∞

c   airfoil chord

1

c_h flap hinge moment coefficient, taken about hinge line, positive in direction of δ_f, (hinge moment)$/q_\infty c^2$

c_l lift coefficient, lift$/q_\infty c$

c_m pitching moment coefficient, taken about $c/4$, positive nose up, moment$/q_\infty c^2$

C_p pressure coefficient, $(p-p_\infty)/q$

C_p^* pressure coefficient for sonic flow

ΔC_p difference in pressure coefficient, $C_{p_{lower}} - C_{p_{upper}}$

Im imaginary or out-of-phase part

k reduced frequency, $\omega c/2V$

k_c reduced frequency of critical or "modal" oscillation

M Mach number

p pressure (dimensional)

q_∞ freestream dynamic pressure $\frac{1}{2}\rho_\infty V_\infty^2$

Re real or in-phase part

t nondimensional time, $\bar{t}/(c/2V_\infty)$

$\bar{t}$ dimensional time, s

Δt nondimensional time step

U (velocity component in x-direction)$/V_\infty$

V (velocity component in y-direction)$/V_\infty$

V_∞ free-stream total velocity (dimensional)

x,y coordinate distances

α angle of attack

2

γ	ratio of specific heats
δ_f	flap deflection, positive trailing edge down
θ	pitch angle, positive nose up
ρ_∞	free-stream density (dimensional)
ϕ	perturbation potential
ω	frequency of oscillation, rad/s

GENERAL DESCRIPTION OF THE METHOD

The potential equation for two-dimensional time-dependent flow is

$$(a^2 - U^2)\phi_{xx} - 2UV\phi_{xy} + (a^2 - V^2)\phi_{yy}$$

$$- 2U\phi_{xt} - 2V\phi_{yt} - \phi_{tt} = 0$$

where

$$\phi = \text{perturbation potential}$$

$$U = \cos\alpha + \phi_x$$

$$V = \sin\alpha + \phi_y$$

$$a^2 = a_\infty^2 - 0.5(\gamma - 1)(2\phi_t + U^2 + V^2 - 1)$$

This equation is nonlinear because a, U, and V are functions of ϕ, and numerical finite difference techniques are generally used to obtain solutions. Use of the full potential equation yields a method that is intermediate in completeness and computational effort between methods that use the Euler equations (ref. 8) and those that use the small disturbance equation (references 9 and 10). One advantage of using the potential equation as compared with the Euler equations is that for the potential equation only the single variable ϕ has to be stored, whereas for the Euler equations ρ, p, U, and V must be stored.

The semi-implicit finite difference technique (ref. 1) is used which alleviates some of the limits on time step required for stability. An unpublished addition to the algorithm of reference 1 has also been made by Isogai which increases the permissible time step. It essentially is an additional implicit pass through the flow field. The time step is still restricted, however, which implies that the computer time increases as reduced frequency k decreases. The method also uses a rotated difference scheme to maintain

numerical stability.

A stretched rectangular Cartesian grid system similar to that of reference 11 is used to map the infinite physical space to a finite computational system. For all calculations presented herein, a 57 x 57 grid system was used, although some calculations using other grid systems are discussed. The upper half of the grid is shown in figure 1 in physical space. One finite y-grid line and the lines at infinity are not shown. The mapping clusters points near the leading and trailing edges and near the airfoil surface, but no special consideration is given to shocks or hinge lines. For the grid system used (fig. 1), there are 29 points on each airfoil surface with the first and last points on the airfoil at 0.01c and 0.99c, respectively. In comparison with conventional steady flow transonic calculations, this grid system might be considered a medium grid rather than a coarse or fine grid system.

The airfoil motion boundary condition is applied at the mean airfoil position. This assumption may restrict the valid range of amplitude of motion but simplifies the computer program because the airfoil and computation grid remain fixed in time. In addition, the finite difference method uses a quasi-conservative shock-capturing difference scheme to treat moving shock waves (ref. 1). This treatment of shock waves ensures that the correct shock jump relations are maintained. It also simplifies the computer program since the moving shocks are treated automatically. They are, however, smeared over a few mesh spaces.

The current version of the computer program is dimensioned for a grid of up to 61 x 61 points. It requires 37 000 (114 K_8) locations of central computer memory. On a CYBER 175, operating under the NOS operating system with the FTN compiler, the program takes about ½ seconds of CPU time for each time step. About 3000 time steps are required to converge for a steady flow case and 1000 to 5000 steps for a typical oscillatory case.

RESULTS AND DISCUSSION

Calculations for M = 0.500

The calculated pressure coefficient for the 64A006 airfoil in steady flow at zero angle of attack is compared with experimental data from reference 5 in figure 2. The theory is generally in good agreement but there is some small deviation from the experimental data over the aft portion of the airfoil.

Calculations for harmonic motion.- The variation of unsteady lift with reduced frequency k for a quarter-chord flap oscillating with an amplitude of 1.5° is shown in figure 3 as calculated from linear theory and from the present finite difference method using the nonlinear full potential equation. Harmonic flap oscillation was assumed, and a time step Δt = .05 was used. For this subsonic case there should be good agreement with linear theory with the possible exception of near k = 0. Although the underlying trend of the nonlinear theory is similar to that of linear theory, there are several severe excursions in the results that are apparently spurious. It is believed that these excursions are introduced by the numerical technique. Examination of

4

the output of the program indicates that, at all points in the flow field, there are oscillations which are in phase. Thus the oscillations appear more nearly like standing waves than traveling waves. At reduced frequencies near the peaks of the oscillations, the unsteady load distribution is shifted in phase near the leading edge such that the primary influence is on c_l. Here c_l is shown as it is a more sensitive indicator than c_m or c_h.

The two theories also give a somewhat different behavior near $k = 0$ where thickness may be more important. However, for the finite difference calculations at $k = 0$, the circulation has been neglected for the far field boundary in all of the calculations of this report. In steady flow, the far field boundary should include the mean circulation. If the circulation is included in the calculations for figure 3, the coefficients increase by about 10%. (Such a result may suggest that the finite difference grid may not be adequate.) Although the far field circulation can be readily included in calculations for $k = 0$, no similar boundary condition is available for time dependent calculations, and it is consistent to neglect it for both steady and unsteady calculations. Note also that the trend of the two methods near $k = 0$ may indicate a somewhat different behavior near $k = 0$, but further definition is required to obtain a conclusive result.

Indicial calculations.- A large number of points were required to define the trends shown in figure 3. The 52 points shown and the steady flow calculation required a significant expenditure of computer resources, particularly for the points at low reduced frequencies. The same finite difference program was also used to generate the response for indicial flap deflection shown in figure 4. The response has the expected overall shape of a jump at $t = 0$ plus a real exponential growth to a steady state value. In addition there are several oscillations of different character that appear in the response. Both this curve and the appearance of the results of figure 3 suggest that the response is somewhat analogous to the response of a multi-mode mechanical system and that such an analogy might be useful in defining the characteristics of the results. The method of reference 7 has been applied to fit the response of figure 4 with a series of complex exponential functions in a least square sense such that the amplitude, phase, frequency, and damping of each "mode" or term in the series is calculated. The fit using 8 terms is shown to be essentially coincident with the transient response in figure 4. The components of the transient lift determined by the 8-term fit are shown in figure 5. The offset or steady state value and the first mode are shown in figure 5a and the oscillatory terms are shown in figure 5b. For a steady state calculation, the rate of approach to convergence would be controlled by mode 2, and there should be no influence on the results after it dies out. For the time-dependent problem, however, these "modes" significantly distort the unsteady forces as shown in figure 3. A further indication of these effects is given in figure 6. The harmonic calculations (from fig. 3) are compared with the lift coefficient calculated from the analytic Fourier transform of the 8-mode fit. Good agreement is obtained with some differences in the higher range of k-values. Calculation of the forces for harmonic motion from the Fourier transform of the indicial response is valid only for linear systems.

5

The response for indicial flap displacement should have a delta function at $t = 0+$ that results from the discontinuous velocity at $t = 0$. This is in contrast to the usual indicial functions for subsonic compressible flow that are traditionally given in terms of an indicial velocity rather than displacement (ref. 12). The delta function for the flap displacement contributes to the unsteady lift at all k-values by

$$\Delta c_1 = i \frac{k}{4M} \tag{1}$$

Equation 1 has been derived in a manner similar to the discussion of reference 12. The results of the transient analysis shown in figure 6 include the addition of this term to the transform of the 8 term fit. The finite difference scheme takes a finite time step at $t = 0$ and thus cannot resolve the details of the transient sufficiently to include the delta function. Note that equation (1) gives a large contribution to the imaginary part of c_1 (1.0 at $k = 2.0$ and $M = 0.5$).

The use of the indicial function and the data reduction technique of reference 7 give essentially the same information as that contained in figure 3 but at a cost comparable to the cost of 2 or 3 low frequency points of figure 3, a substantial savings. It appears that potential problems with difference techniques can be analyzed economically in this manner. The additional variable of time makes a global verification of a program of this type a significantly larger task than that for a similar steady flow program.

Relationship to numerical stability.- The question arises as to the relationship of the oscillations to the time step limited stability criterion. A transient for a marginally unstable case is shown in figure 7 which is for a $\Delta t = 0.09825$, about twice the $\Delta t = 0.05$ used previously. The first portion of the curve is qualitatively very similar to that of figure 4 (allowing for the difference in time scale). The latter part of the curve, however, (fig. 7) shows a very rapid divergence with some small high frequency oscillations superimposed. Thus it appears that the modes previously discussed are not those involved in the numerical instability, but rather a static "divergence" is involved. In contrast, the difference scheme of reference 1 goes unstable in an oscillatory fashion at 2/3 of the Nyquist frequency, $k = 2/3 \ (\frac{\pi}{\Delta t})$. The additional smoothing pass of the present method apparently suppresses the high frequency instability and thus increases the allowable time step.

Effects of Various Parameters on Oscillations

To define further some aspects of the oscillations, parameters such as time step, finite difference grid, and Mach number have been explored. As discussed previously, much of the transient response at $M = 0.5$ was essentially the same for $\Delta t = 0.05$ and for $\Delta t = 0.09825$. This situation was also the case for smaller time steps except very near $t = 0$, and the results appear to be remarkably insensitive to time step.

6

Calculations have been made with the number of points used in the finite difference grid reduced by half in the x-direction, half in the y-direction, and by half in both directions. Reducing the number of points in the x-direction had only a modest influence on the frequencies of the oscillations. However, with only half the points in the y-direction, the frequencies of the oscillations were approximately twice the frequencies obtained with the full grid. Reducing the number of points in both directions also doubled the frequencies of oscillations. It appears therefore that the present results are a strong function of the y-grid, and further investigation is needed.

The transonic perturbation method of reference 9 has had considerable difficulty with frequency limitations that have prevented meaningful solutions using conventional relaxation methods except for low values of k. Recently, it has been found that by solving the large system of simultaneous linear equations with an out-of-core solver, good results can be obtained. Frequency limitations can still be encountered, but they are very sensitive to the y-grid arrangement and can be alleviated by the proper choice of finite difference grid. This finding is consistent with the present results for a time dependent method.

Calculated results for a 1° pitching oscillation are shown in figure 8 for a range of reduced frequency up to k = 0.5. Similar deviations occur at the same reduced frequency as for the oscillating flap.

The frequencies of oscillations k_c have been determined for several Mach numbers by using the indicial response, inspecting the Fourier transform for peaks and by fitting with complex exponentials in a manner similar to the calculations M = 0.5. The resulting frequencies are shown in figure 9. For the lower Mach numbers, the frequencies follow an orderly pattern and decrease with Mach number. The damping of the oscillations tends to increase with Mach number, particularly for the higher frequencies, so that there are relatively fewer identifiable frequencies above M = 0.8. Furthermore, in the transonic range for M = 0.85 or higher, shock waves tend to invalidate the linear assumptions. For M = 0.8 to 0.9, the method may be limited to values of k larger than the values of k_c shown as symbols in figure 9.

Calculations for M = 0.875

Steady flow calculations.- The calculated steady pressure coefficient for the 64A006 airfoil is compared with experimental values (ref. 6) in figure 10. The calculated shock wave is stronger and further aft than the experimental one and is fairly near the hinge line at .75c.

The corresponding flap hinge moment for static deflections, shown in figure 11, indicates a strong nonlinearity. As flap deflection is increased, the slope of the curve is initially positive (unstable), rapidly changes to a large stable value, and then levels out. This nonlinear behavior is brought about by the movement of the shock over the upper surface of the flap as the flap deflection is increased and is illustrated by the pressure distributions of figure 12(a)-12(c). Initially, as a result of the relative movement of

7

the upper and lower surface shock waves, there is a small down load over the flap (fig. 12a). At an intermediate deflection level, there is a large effect on the loading of the flap and airfoil as the upper surface shock moves aft over the airfoil and the lower one moves forward (fig. 12b). However, once the upper surface shock reaches the trailing edge, there is decreased effectiveness as only the loading over the flap is changed. Although this trend may not be accurately predicted by the present method (since shock wave strength is overpredicted) such a phenomenon would be anticipated to occur for conditions that lead to movement of a shock over the control surface. In practice, however, these trends might also be altered significantly by boundary layer effects. This case illustrates a phenomenon that should be interesting to investigate more fully, particularly considering its aeroelastic implications.

Unsteady calculations.- The transient lift for an indicial flap displacement of 1.5° corresponding to this nonlinear static behavior is shown in figure 13. There is a considerable change in character from that at $M = 0.5$ (fig. 4). The initial portion is nearly linear and then a spike or corner occurs, apparently as a result of shock motions. The latter portion of the response again involves an oscillatory behavior. The exponential series fits the response well except near the corner or spike.

Oscillatory results calculated from harmonic motion are compared with linear theory in figure 14. The nonlinear results approach the linear results at the higher k-values, but there are again large oscillations of the unsteady lift with reduced frequency in the results of the finite difference calculations. Although the results would not be expected to agree with linear theory at low reduced frequencies, these oscillations are not considered to be physical but introduced by the numerical method. In particular, the result at $k = 0.059$ is near one of the frequencies extracted from the transient response. It might be noted that these results at $M = 0.875$ smooth out much more rapidly with k (fig. 14) than do the results of $M = 0.5$ (fig. 3).

The unsteady coefficients have also been calculated from the Fourier transform of the computed fit to the indicial response and are compared with the calculations for harmonic oscillations (1.08° flap amplitude) in figure 15. Although the two results are somewhat similar in character, they do not agree well at low reduced frequencies. The transform process depends on linearity and the static forces are quite nonlinear in this case (fig. 11). The indicial response and its tranform however would be a good indicator of possible problems with the difference method.

CONCLUDING REMARKS

Extensive calculations with a semi-implicit method for solving the two-dimensional unsteady full potential equation have indicated that the numerical technique as presently formulated generates spurious oscillations in the indicial response functions and in the corresponding aerodynamic coefficients versus reduced frequency. These oscillations appear to be related to the spatial finite difference grid, and further development is needed to improve the accuracy of the method.

8

An extensive computational effort is required to verify a time dependent program such as the one discussed herein, but this effort can be reduced through the use of indicial methods. In the present investigation, the use of conventional dynamic data analysis methods of Fourier transforms and of time-plane fitting with complex exponentials was helpful in determining the existence and trends of the oscillations.

REFERENCES

1. Isogai, Koji: Calculation of Unsteady Transonic Flow over Oscillating
    Airfoils Using the Full Potential Equation. AIAA/ASME 18th Structures,
    Structural Dynamics and Materials Conference, Vol. B (San Diego,
    California), March 1977, pp. 245-256.

2. Isogai, Koji: Numerical Study of Transonic Flow over Oscillating Airfoils
    Using the Full Potential Equation. NASA TP-1120, 1978.

3. Bennett, Robert M.; and Bland, Samuel R.: Some Calculations of Transonic
    Potential Flow for the NACA 64A006 Airfoil with an Oscillating Flap.
    In, Advanced Technology Airfoil Research, NASA CP-2045, Vol. I, Part 2,
    pp. 689-700, March 1979.

4. van der Vooren, J.; Slooff, J. W.; Huizing, G. H.; and van Essen, A.:
    Remarks on the Suitability of Various Transonic Small Perturbation
    Equations to Describe Three Dimensional Transonic Flow; Examples of
    Computations Using a Fully Conservative Rotated Difference Scheme.
    In, Symposium Transonicum II, pp. 557-566, Springer Verlag, New York,
    1976.

5. Tijdeman, H.; and Schippers, P.: Results of Pressure Measurements on
    an Airfoil with Oscillating Flap in Two-Dimensional High Subsonic and
    Transonic Flow (Zero Incidence and Zero Mean Flap Position). NLR
    TR 73078 U, Nat. Lucht - Ruimtevaartlab. (Amsterdam), July 13, 1973.

6. Tijdeman, H.; and Schippers. P.: Results of Pressure Measurements on a
    Lifting Airfoil with Oscillating Flap in Two-Dimensional High Subsonic
    and Transonic Flow. NLR TR 73018 L, Nat. Lucht - Ruimtevaartlab.
    (Amsterdam), Nov. 1974.

7. Bennett, Robert M.; and Desmarais, Robert N.: Curve Fitting of Aeroelastic
    Transient Response Data with Exponential Functions. In, Flutter Testing
    Techniques. NASA SP-415, pp. 43-58, 1976.

8. Magnus, R. J.: Calculations of Some Unsteady Transonic Flows About the
    NACA 64A006 and 64A010 Airfoils, AFFDL-TR-77-46, U.S. Air Force, July 1977.

9. Weatherill, Warren H.; Sebastian, James D.; and Ehlers, F. Edward: The
    Practical Application of a Finite Difference Method for Analyzing Tran-
    sonic Flow over Oscillating Airfoils,and Wings. NASA CR-2933, 1978.

10. Ballhaus, W. F.; and Goorjian, P. M.: Implicit Finite-Difference Compu-
    tation of Unsteady Transonic Flows About Airfoils. AIAA J., vol. 15,
    no. 12, Dec. 1977, pp. 1728-1735.

11. Carlson, Leland, A.: Transonic Airfoil Flowfield Analysis Using Cartesian
    Coordinates. NASA CR-2577, 1975.

12. Bisplinghoff, Raymond L.; Ashley, Holt; and Halfman, Robert L.: Aeroelasticity. Addison-Wesley Publishing Co., Inc., Reading, Massachusetts, 1955.
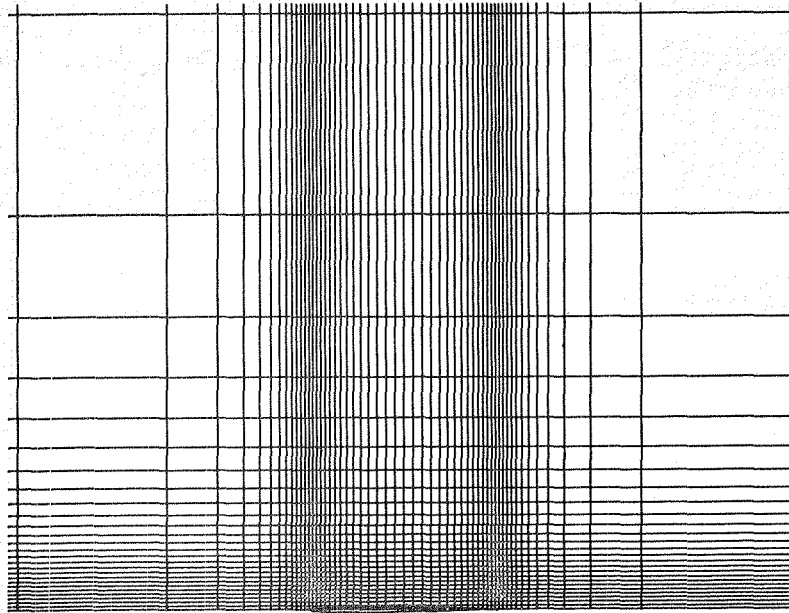
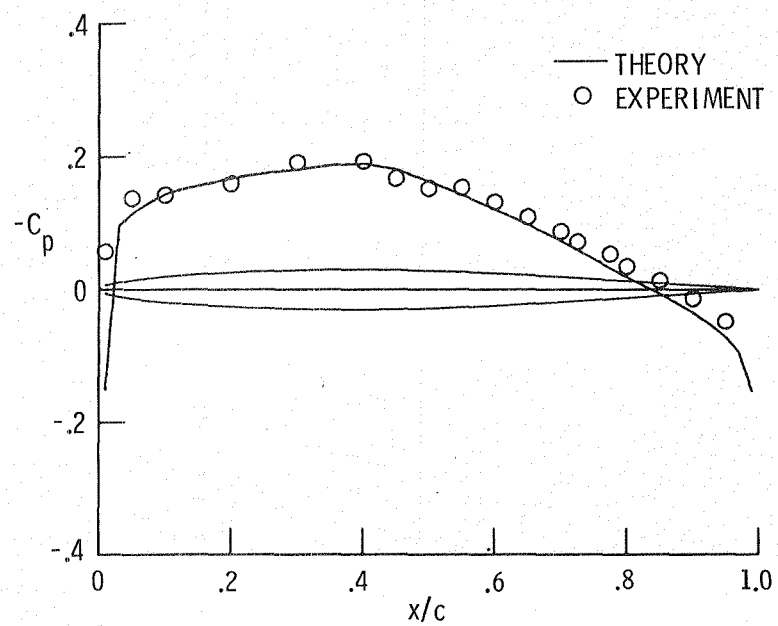Figure 1.- Grid system used in calculations,
57 x 57.

Figure 2.- Steady pressure distribution for the
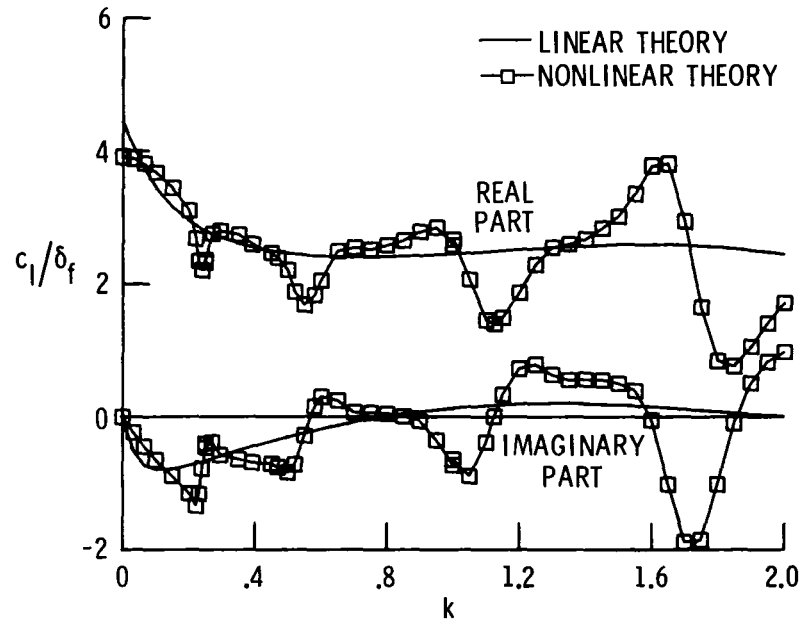NACA 64A006 airfoil at $M = 0.5$ and $\alpha = 0$.

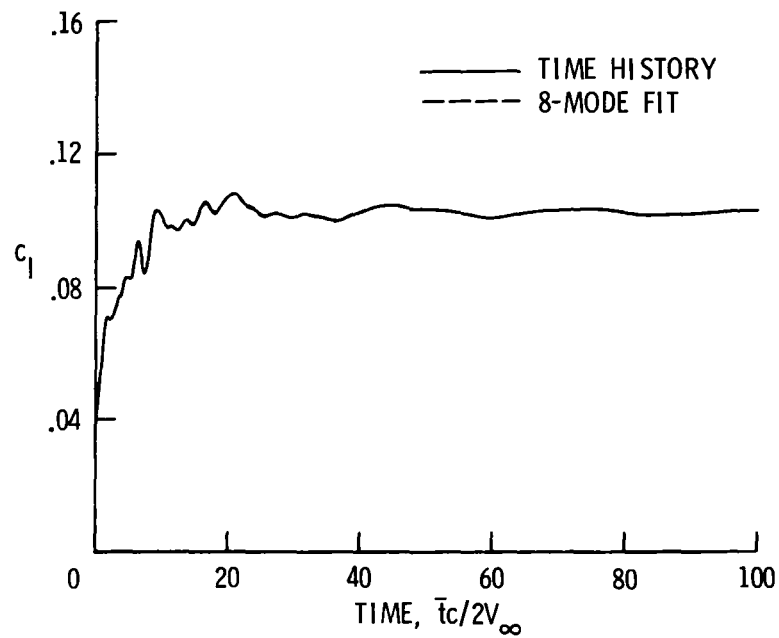Figure 3.- Unsteady lift due to flap motion at
$M = 0.5$ and $\alpha = 0$.

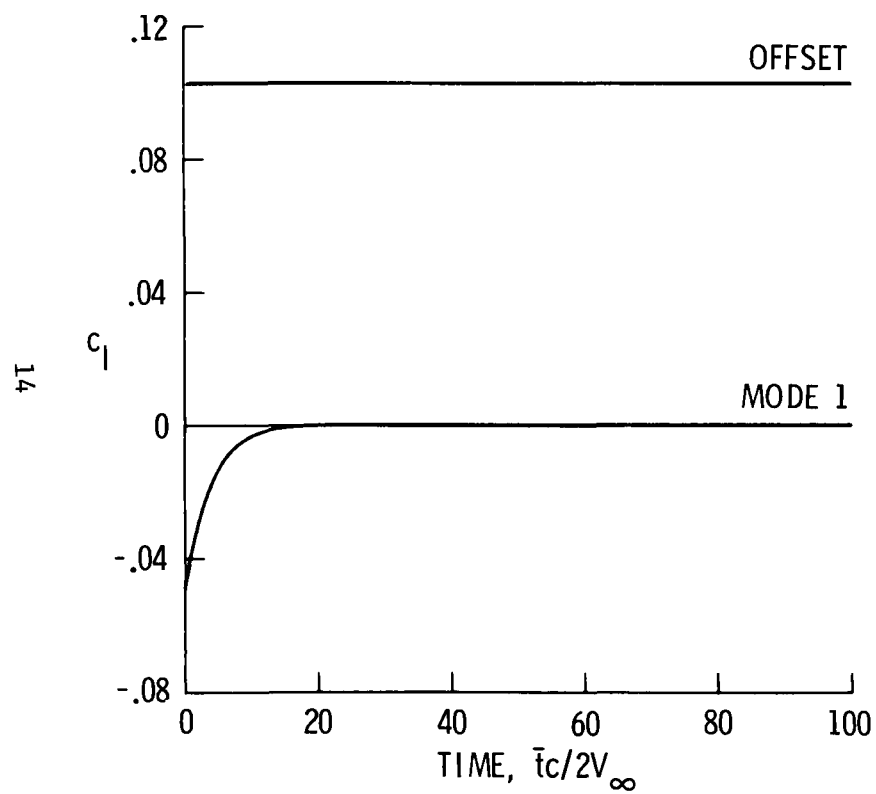Figure 4.- Transient lift for a 1.5^O step in flap
deflection at $M = 0.5$ and for $\Delta t = 0.05$.

Figure 5.- Components of transient lift for 1.5^0 step in flap deflection at $M = 0.5$.

(a) Offset and mode 1.
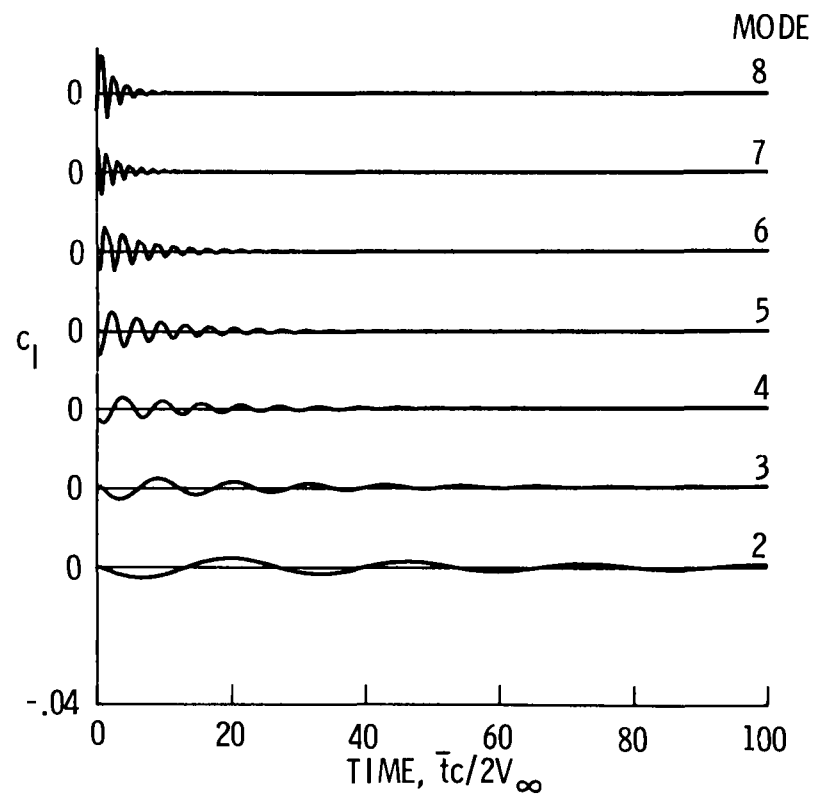
Figure 5.- Concluded.

(b) Modes 2 through 8.

14
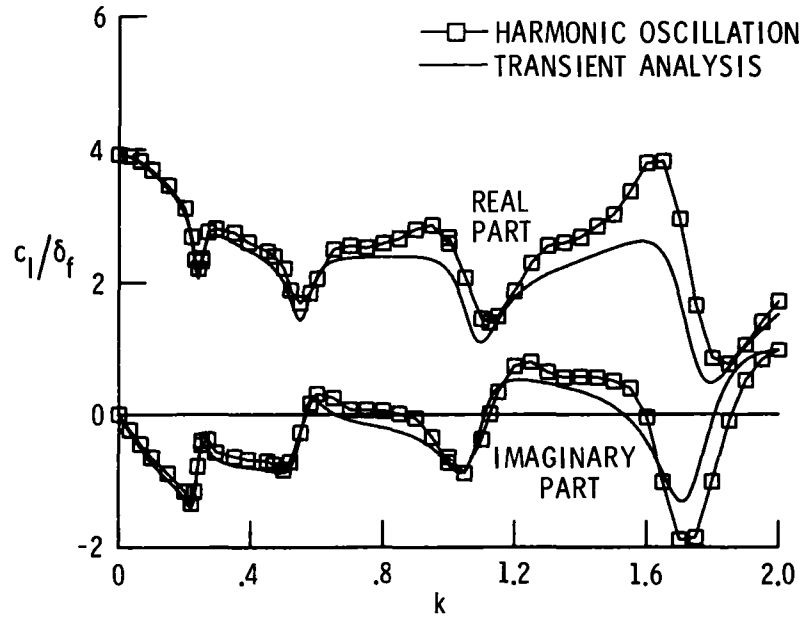
Figure 6.- Comparison of harmonic and transient analyses for lift due to flap motion at $M = 0.5$ and $\alpha = 0$.
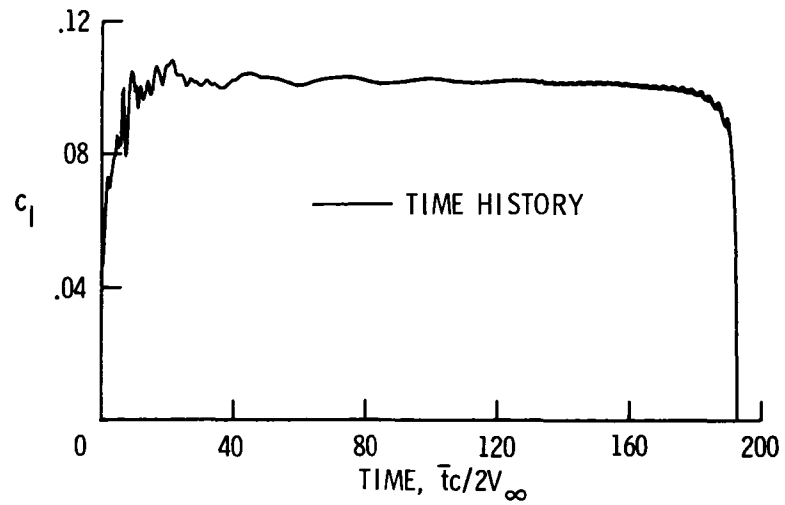
Figure 7.- Transient lift for 1.5° step in flap deflection at $M = 0.5$ and for $\Delta t = 0.09825$.
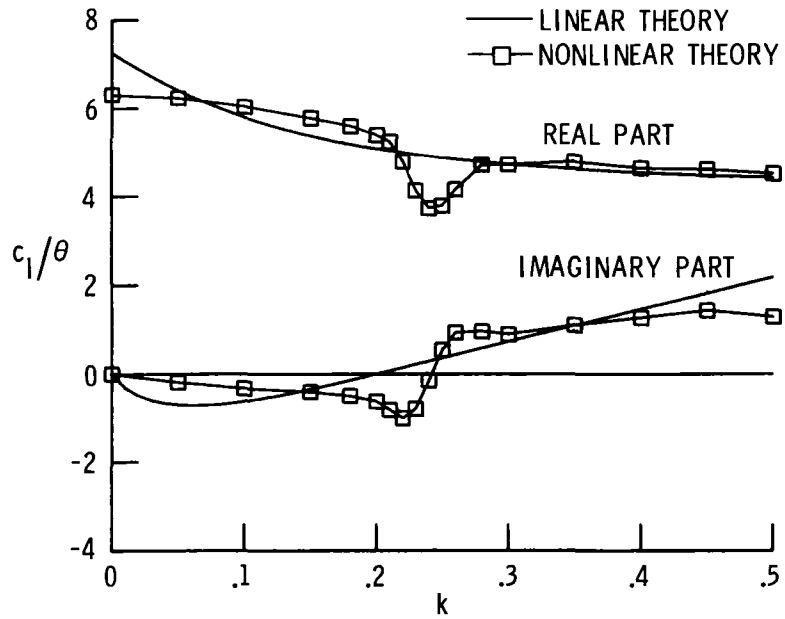
Figure 8.- Unsteady lift due to pitching motion
for M = 0.5 and α = 0.
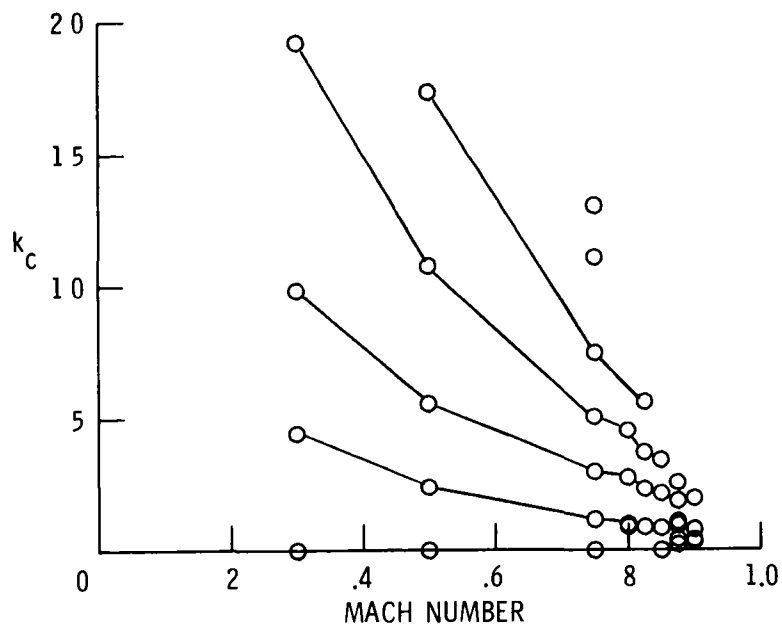
Figure 9.- Frequencies identified in transient
data.

16
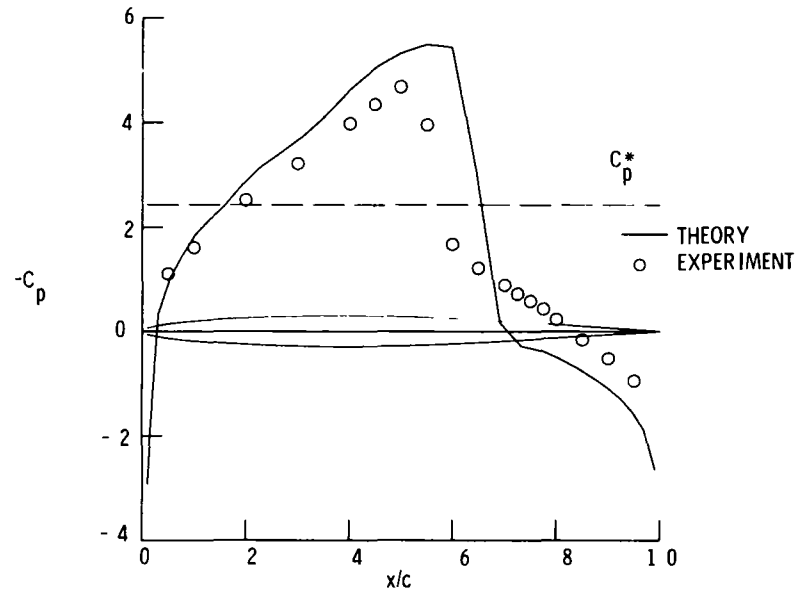
Figure 10.- Steady pressure distribution for the
NACA 64A006 airfoil at M = 0.875 and α = 0.
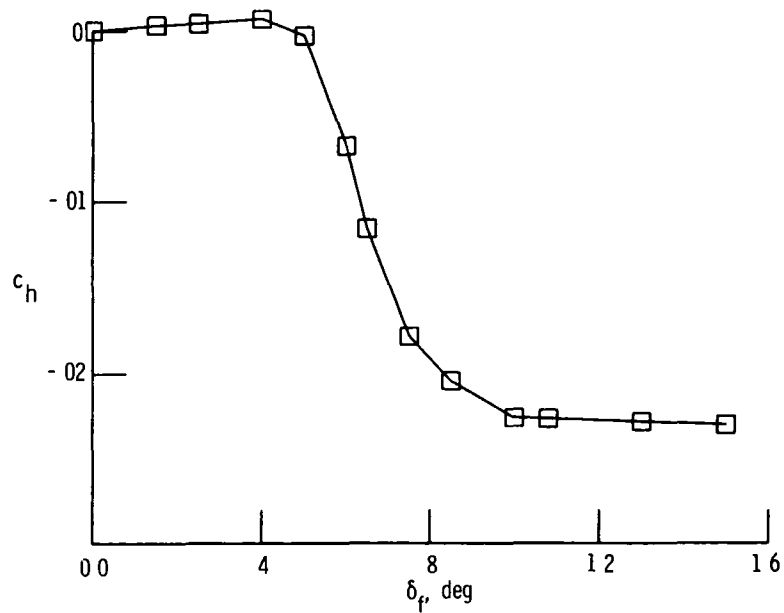
Figure 11.- Steady hinge moment due to flap
deflection for the NACA 64A006 airfoil at
M = 0.875 and α = 0.
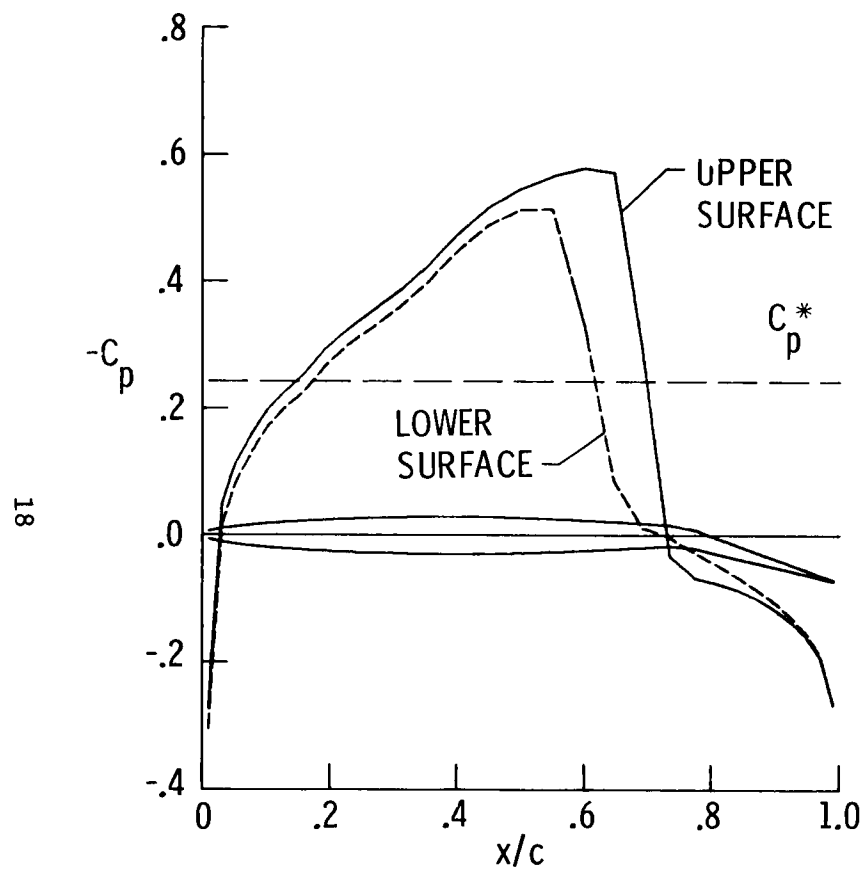
Figure 12.- Steady pressure distribution for the
NACA 64A006 airfoil at M = 0.875 and α = 0.

(a) δ_f = 0.15°
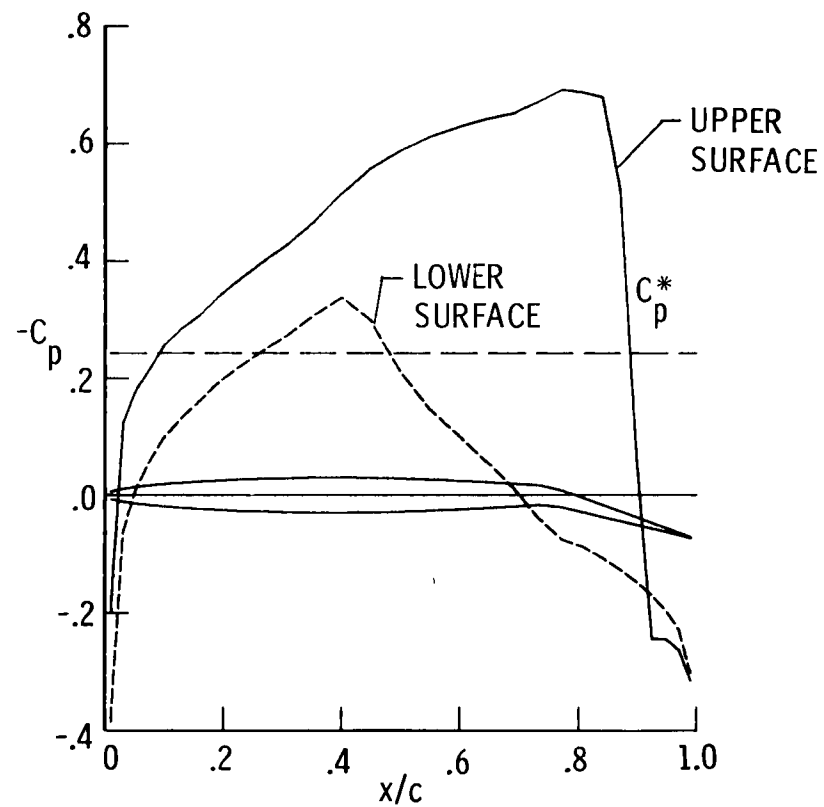
Figure 12.- Continued.

(b) δ_f = 0.60°

18
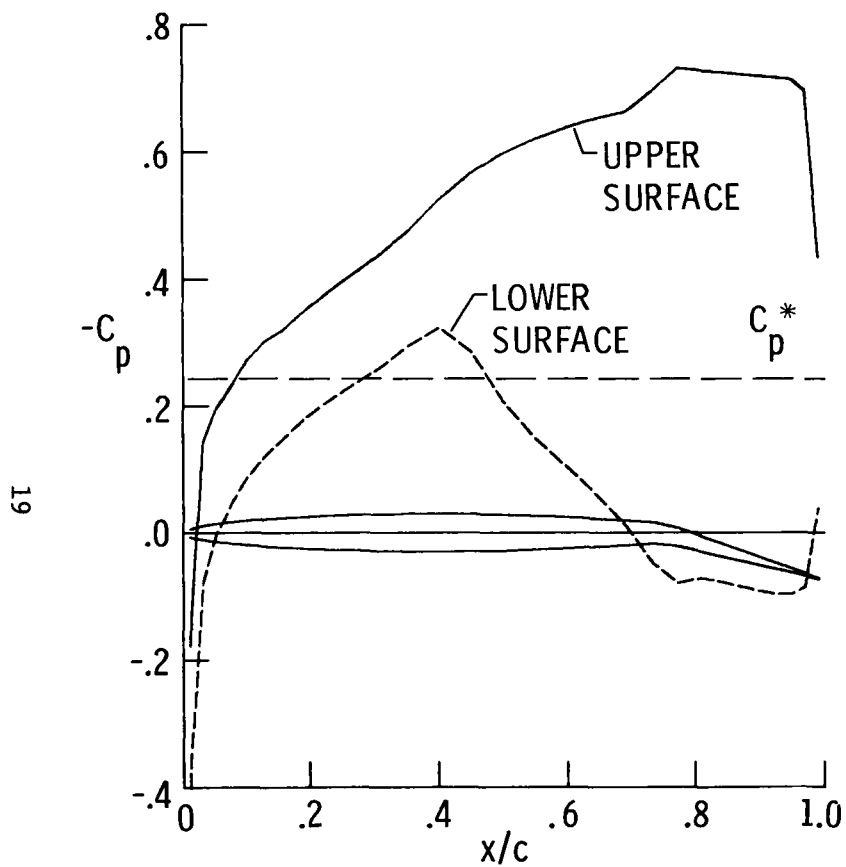
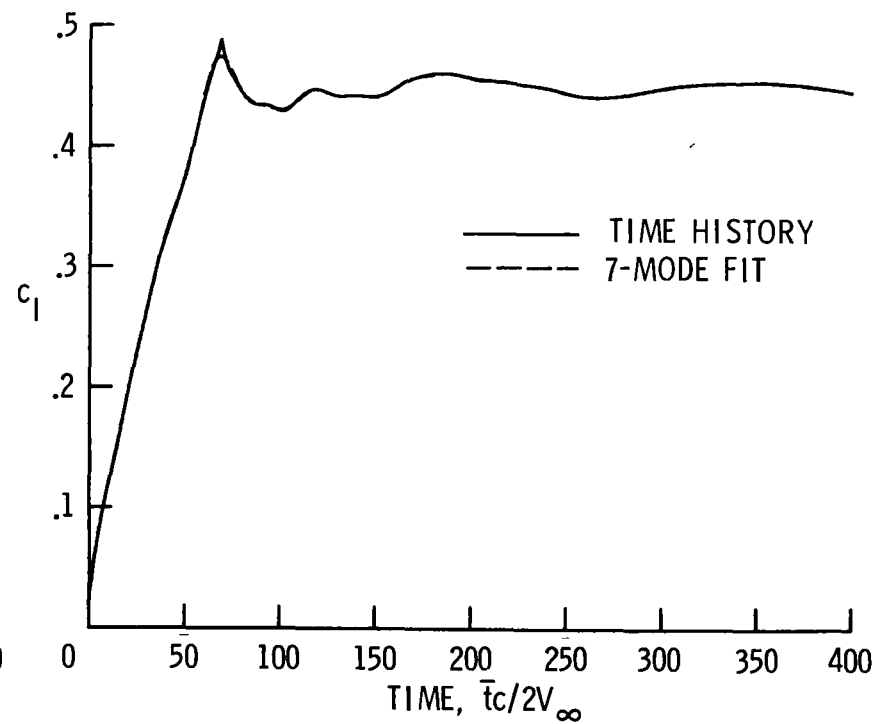Figure 12.- Concluded.

(c) $\delta_f = 1.08^o$

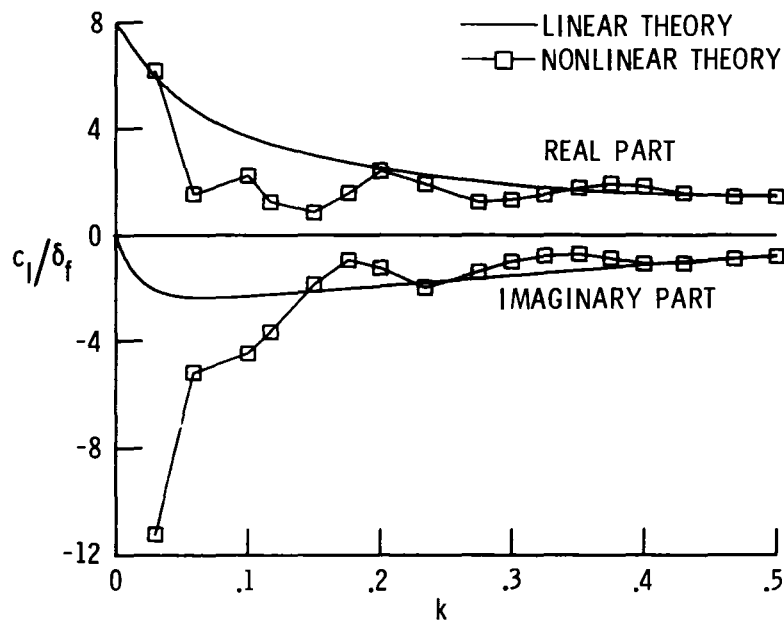Figure 13.- Transient lift for a 1.5^o step in flap deflection at $M = 0.875$ and for $\Delta t = 0.11$.

Figure 14.- Unsteady lift due to flap motion at
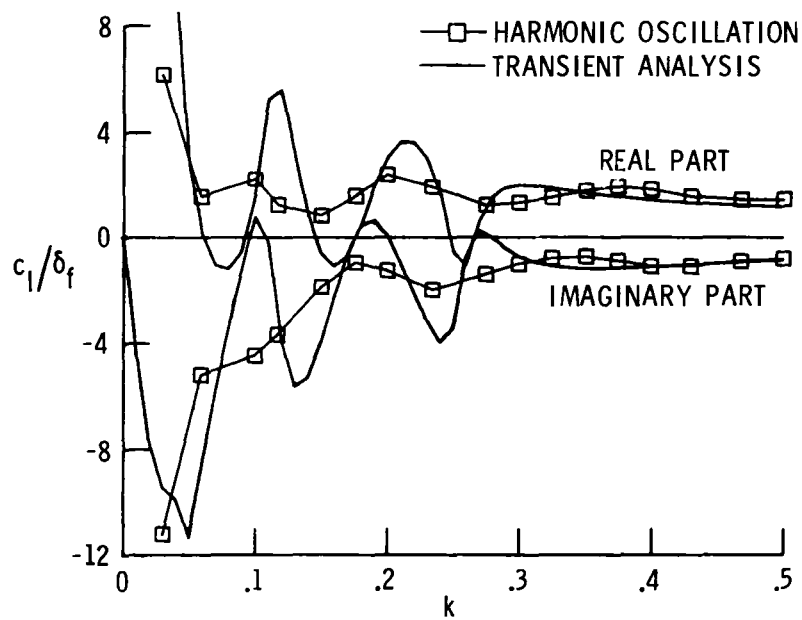M = 0.875 and α = 0.

Figure 15.- Comparison of harmonic and transient
analyses for lift due to flap motion at M = 0.875
and α = 0.

End of Document